



Article

A Study of Catalytic Oxidation of a Library of C₂ to C₄ Alcohols in the Presence of Nanogold

Maciej Kapkowski ¹, Anna Niemczyk-Wojdyla ¹, Piotr Bartczak ¹, Monika Pyrkosz-Bulska ¹, Kamila Gajcy ¹, Rafal Sitko ¹, Maciej Zubko ^{2,3}, Jacek Szade ⁴, Joanna Klimontko ⁴, Katarzyna Balin ⁴ and Jaroslaw Polanski ^{1,*}

¹ Institute of Chemistry, University of Silesia, Szkolna 9, 40-006 Katowice, Poland; maciej.kapkowski@us.edu.pl (M.K.); anna.niemczyk@us.edu.pl (A.N.-W.); piotr.bartczak@us.edu.pl (P.B.); monika.pyrkosz-bulska@us.edu.pl (M.P.B.); kamila.gajcy@us.edu.pl (K.G.); rafal.sitko@us.edu.pl (R.S.)

² Institute of Materials Science, University of Silesia, 75 Pułku Piechoty 1A, 41-500 Chorzów, Poland; maciej.zubko@us.edu.pl

³ Department of Physics, University of Hradec Králové, Rokitanského 62, 500-03 Hradec Králové, Czech Republic

⁴ Institute of Physics, University of Silesia, 75 Pułku Piechoty 1A, 41-500 Chorzów, Poland; jacek.szade@us.edu.pl (J.S.); joanna.klimontko@us.edu.pl (J.K.); katarzyna.balin@us.edu.pl (K.B.)

* Correspondence: jaroslaw.polanski@us.edu.pl; Tel.: +48-32-2599978

Received: 26 January 2019; Accepted: 12 March 2019; Published: 15 March 2019



Abstract: The classical stoichiometric oxidation of alcohols is an important tool in contemporary organic chemistry. However, it still requires huge modifications in order to comply with the principles of green chemistry. The use of toxic chemicals, hazardous organic solvents, and the large amounts of toxic wastes that result from the reactions are a few examples of the problems that must be solved. Nanogold alone or conjugated with palladium were supported on different carriers (SiO₂, C) and investigated in order to evaluate their catalytic potential for environmentally friendly alcohol oxidation under solvent-free and base-free conditions in the presence H₂O₂ as a clean oxidant. We tested different levels of Au loading (0.1–1.2% wt.) and different active catalytic site forms (monometallic Au or bimetallic Au–Pd sites). This provided new insights on how the structure of the Au-dispersions affected their catalytic performance. Importantly, the examination of the catalytic performance of the resulting catalysts was oriented toward a broad scope of alcohols, including those that are the most resistant to oxidation—the primary aliphatic alcohols. Surprisingly, the studies proved that Au/SiO₂ at a level of Au loading as low as 0.1% wt. appeared to be efficient and prospective catalytic system for the green oxidation of alcohol. Most importantly, the results revealed that 0.1% Au/SiO₂ might be the catalyst of choice with a wide scope of utility in the green oxidation of various structurally different alcohols as well as the non-activated aliphatic ones.

Keywords: nanogold catalysis; nanomaterials; alcohol oxidation; hydrogen peroxide; silicon dioxide; green chemistry

1. Introduction

Large amounts of alcohols can be obtained from natural and renewable sources. Therefore, they are attractive starting materials for the chemical industry. In particular, the oxidation of alcohols into their corresponding carbonyl compounds is one of the most important organic transformations because of the high value of these products in the manufacture of fine chemicals, pharmaceuticals, and special materials [1]. The classical methods of alcohol oxidation involve the use of stoichiometric amounts of toxic oxidants (such as chromates and permanganates), harmful organic solvents, and vigorous reaction

conditions [2]. With the intensively growing environmental concerns and more stringent ecological standards in industry, there is an emerging quest to develop economic and efficient “green” processes for alcohol oxidation. Recently, the catalytic oxidation of alcohols that have a reusable catalytic system and environmentally benign oxidants such as O_2 and H_2O_2 have received considerable attention owing to its low environmental impact, especially when compared to stoichiometric oxidation [3].

Gold-assisted catalysis is one of the fastest growing research topics in the field of catalysis, including the area of catalytic oxidation. Although gold has been regarded as being catalytically inert for centuries, studies in the 1980s revealed that nanogold particles (NPs) display an exceptional catalytic activity at low temperatures, especially in the oxidation reaction [4]. The pioneering work of Haruta et al. [4] showed that ultrafine (~5 nm) Au particles that were supported on Fe_2O_3 , Co_3O_4 , and NiO had a high level of activity in the low-temperature aerobic oxidation of carbon monoxide. This phenomenon has never been reached by other metals [5]. Following this outstanding finding, gold nanoparticles were used in the oxidation of alcohols into aldehydes, carboxylic acids, or esters; in the oxidation of aldehydes to esters or acids into epoxidations of olefins; and in the oxidation of amines into amides [6]. Recently, it has further been found that compared to platinum catalysts, nanogold catalysts feature higher level of activity, a higher selectivity, and a better stability for the liquid-phase oxidation of various alcohols [7]. Furthermore, the use of nanogold catalysts instead of platinum catalysts can be particularly advantageous in the case of the application of alcohol oxidation in the manufacture of active pharmaceutical ingredients (APIs). The platinum group metals are classified as “substances of significant concern”, which have residues of APIs < 10 ppm when administered orally, while gold has a limited toxicity [8]. Furthermore, gold is considerably more abundant and cheaper than the platinum group metals [9]. The unique properties of gold nanoparticles make them highly attractive in the development of novel sustainable catalytic systems for alcohol oxidation, which could be particularly suitable for industrial applications.

In the present work, a series of nanogold dispersions were prepared in order to examine their catalytic potential in the oxidation of alcohols under environmentally benign conditions. It is well known that the catalytic activity of gold catalysts is primarily determined by the particle size of Au, the properties of the support material and the method that is used to prepare the catalyst [10]. Herein, the properties of the nanogold catalysts were adapted by changing the support materials, using different levels of Au loading and incorporating a second metal in order to form a bimetallic structure.

It is well known that a number of catalysts display a high level of activity for the oxidation of specific types of alcohols [11]. For examples, Biffis et al. [12] reported that microgel-stabilized Pd nanoclusters are effective for the oxidation of secondary alcohols, while Abad et al. [13] showed that ceria-supported Au nanoparticles are most suitable for the oxidation of allylic alcohols and can prevent the isomerization and hydrogenation of the C=C double bonds.

By contrast, the aim of our studies was to find a catalytic system that can activate a wide range of substrates, including nonactivated aliphatic alcohols that can be used under mild conditions. In the model reactions, a green methodology was developed that can oxidize alcohols. In the first experiment, hydrogen peroxide was applied as the oxidant. This ‘clean’ oxidant did not produce any toxic or waste side-products and produced water as the only by-product. In the second experiment, the model reactions were carried out under solvent- and base-free conditions, in which some practical problems such as further product purification, waste base treatment, and the disposal cost of harmful wastes can be overcome.

2. Materials and Methods

2.1. Catalyst Preparation

2.1.1. The Nanodispersion of Au and Pd/SiO₂

A silica carrier was synthesized using the Stöber method with tetraethyl orthosilicate (TEOS (99.0%), Sigma Aldrich, St. Louis, MO, USA) as the silica source. The procedure was as follows:

1500 mL of anhydrous methanol (99.8%, Sigma Aldrich, St. Louis, MO, USA) and 528 mL of an ammonia solution (25 wt. %, Chempur, Piekary Śląskie, Poland) were mixed with 305 mL of deionized water, and then the mixture was stirred for 10 min. Next, 100 g of TEOS was added to the reaction mixture, which was then stirred for 5 h at room temperature. The colloidal suspension was centrifuged and then placed in an ultrasound bath and stirred for 90 min. The resulting precipitate was washed with distilled water until neutral pH was reached. In the next step, a solution of 30% H₂AuCl₄ or PdCl₂ (POCH, Gliwice, Poland), or both (Table S1), in deionized water (10 mL) was added dropwise onto the silica carrier that had been obtained and stirred for 30 min. Then, it was dried at 60–90 °C for 12 h in the dark, ground, and sieved. Finally, without calcination a reduction of the obtained products was conducted in an oven at 500 °C for 4 h under a hydrogen atmosphere. After reduction the oven was cooled to 25 °C and purged with nitrogen for 15 min. The catalyst was stored in a gas-tight container.

2.1.2. Nano-Dispersion of Au/C

The general procedure was as follows: Dispersion of 0.7% AuNPs/SiO₂ (4.0 g) from Experiment 2.1.1 and the target carrier, i.e., C (14.0 g), were suspended in deionized water (80 mL) under mechanical stirring (BOS, Stargard, Poland) and sonication (Bandelin Sonorex, Berlin, Germany). After 10 min of vigorous stirring, sodium hydroxide (23.3 mL 40% w/w) was added to the suspension and the stirring was continued for 2 h at room temperature. Then, the suspension was allowed to stand for about 18 h until the suspended solid sedimented. In the next step, the suspension was centrifuged and the supernatant was decanted. The resulting precipitate was washed eight times with deionized water and centrifuged again to achieve neutral pH of the supernatant, which was then removed. The second generation precipitate was washed with deionized water, centrifuged, and the supernatant was removed. The catalyst that was obtained was dried in an electric dryer at 120 °C in order to get a constant weight.

2.2. Methods for the Characterization of the Catalyst

An energy dispersive X-ray fluorescence (EDXRF) analysis of the catalysts was performed on an Epsilon 3 spectrometer (Panalytical, Almelo, The Netherlands) with a Rh target X-ray tube that was operated at a maximum voltage of 30 keV and a maximum power of 9 W. This spectrometer is equipped with a thermoelectrically cooled silicon drift detector (SDD) that has an 8 μm Be window and a resolution of 135 eV at 5.9 keV. The quantitative analysis was performed using Omnian software and was based on the fundamental parameter method.

The powder X-ray diffraction (XRD) experiments of the catalysts were performed on a (Panalytical, Almelo, The Netherlands) that was equipped with a pixel detector using Cu K α radiation at 40 kV and 30 mA. The diffractograms were registered in the 10°–140° 2 θ angle range at 0.0131° steps. A qualitative phase analysis was performed using the “X’Pert High Score Plus” computer program and the diffractograms that were obtained were compared to the standard database of the International Centre for Diffraction Data (ICDD).

The transmission electron microscopy (TEM) observations were performed using a JEOL (JEOL Ltd., Tokyo, Japan) high resolution (HRTEM) JEM 3010 microscope operating at a 300 kV accelerating voltage and equipped with a Gatan (Gatan, Inc., Pleasanton, CA, USA) 2k × 2k OriusTM 833SC200D CCD camera and an EDS detector from IXRF (IXRF Systems Inc., Austin, TX, USA). The samples were suspended in isopropanol and the resulting materials were deposited on a Cu grid that had been coated with an amorphous carbon film that was standardized for TEM observations. The size distribution of the nanoparticles was calculated from the recorded TEM images. For the AuPd/SiO₂ catalyst sample, 540 metallic nanoparticles were considered in the calculations. The concentration of nanoparticles for the 0.1% Au/SiO₂ catalyst sample was significantly lower, and therefore only approximately 40 nanoparticles were used to determine the size distribution. Nevertheless, because the nanoparticles were more homogeneous, the lower amount of particles seems to be reasonable for obtaining good size distribution statistics.

The resulting preparations of silica or carbon-supported catalysts were examined with a Prevac/VGScienta photoelectron spectrometer (R3000 electron spectrometer, VG Scienta AB, Uppsala, Sweden and PREVAC sp. z o.o., Rogow, Poland) using X-ray photoelectron spectroscopy (XPS). Monochromatic AlK α x-ray radiation ($h\nu = 1486.7$ eV) was used to obtain the photoelectron spectra of the core levels of specific elements. The structure of the XPS multiplets that were obtained was analyzed using the Multipak program (PHI Multipak SoftwareTM Version 9.6.0.15, 2015.02.19, Ulvac-phi Inc., Chigasaki, Kanagawa, Japan) from Physical Electronics.

2.3. Alcohol Oxidation

Aliphatic monoalcohols (i.e., ethanol, 1-propanol, 2-propanol, and 2-butanol) as well as diols (i.e., 1,2-ethanediol, 1,2-propanediol, 1,3-propanediol, and 2,3-butanediol) were used as the model alcohols for the catalytic oxidation. The resulting nano-Au catalyst (20 mg, 0.1–1.9 μ mol of Au) was suspended in a mixture of 30% H₂O₂ (1.0 mL, 9.8 mmol H₂O₂) and 0.5 mL of alcohol (1.0 mol/L, 0.5 mmol). Then, the suspension was agitated for 10 min. using a sonication bath (RK 52 H, Bandolin Electronics, 35 kHz). In the next step, the solution was stirred at 300 rpm in a sealed tube (septa system) that was placed in a thermostatic oil bath at 85 °C for 20 h. The reaction mixture was centrifuged and decanted. The supernatant was dissolved in deuterium oxide and analyzed using ¹H and ¹³C NMR. Additionally, the 2D COSY and HMQC methods were used to identify and quantify the products. The NMR spectra were recorded on Bruker Avance 400 or Bruker Ascend 500 spectrometers (Bruker, Karlsruhe, Germany) with TMS as the internal standard (400 MHz ¹H, 101 MHz ¹³C or 500 MHz ¹H, 126 MHz ¹³C) at room temperature. The signal from the water was suppressed using 90 water-selective pulses. Exemplary NMR spectra with the products of the alcohol oxidation are presented in Figures S1 and S2. Equations (1)–(5) were used to calculate the conversion, product selectivity, yield, turnover number (TON), and turnover frequency (TOF), respectively.

$$\text{Conversion}(\%) = \frac{(\text{initial moles of alcohol} - \text{final moles of alcohol})}{\text{initial moles of alcohol}} \times 100 \quad (1)$$

$$\text{Selectivity of products}(\%) = \frac{\text{percentage amount of product formed}}{\text{the total percentage of all product formed}} \times 100 \quad (2)$$

$$\text{Yield}(\%) = \frac{\text{conversion of alcohol} \times \text{selectivity of desired product}}{100} \quad (3)$$

$$\text{TON} = \frac{\alpha \cdot n_{\text{sub}}}{n_{\text{met}}} \quad (4)$$

$$\text{TOF} = \frac{\text{TON}}{t} \left[\text{h}^{-1} \right] \quad (5)$$

where n_{sub} is the total number of moles of substrate, n_{met} is the number of moles atoms of nanometal/s, t is the time in hours, and α is the system conversion degree.

3. Results and Discussion

A set of five different nanogold dispersions were prepared and characterized in order to perform comparative studies on their catalytic performance in the liquid phase oxidation of alcohols. Taking into account the fact that different preparation methods can lead to different structural properties of the catalysts, we used the same technique to prepare all of the catalysts that were examined [14]. The method for preparing the catalyst was developed, proven experimentally, and previously reported [15]. The physiochemical properties of the nanogold catalysts were modified by the following changes: the type of material for the catalytic support and the level of Au-loading as well as coupling the Au with another metal in order to form bimetallic active centers instead of monometallic ones. It was assumed that a combination of these factors might affect the final properties of the resulting catalysts in many ways.

3.1. Characterization of the Catalysts

The EDXRF spectra of (0.2% Pd; 1.1% Au)/SiO₂ and (1.1% Pd; 0.4% Au)/SiO₂ are presented in Figure 1. The spectra show Au lines (L α , L β , L γ at 9.71, 11.44 and 13.38 keV, respectively), Pd lines (L α and L β at 2.84 and 2.99 keV, respectively), as well as a K α Si line at 1.74 keV. The results of the EDXRF and XPS analyses were compared with the actual values of the Au- and Pd-loading in Table 1.

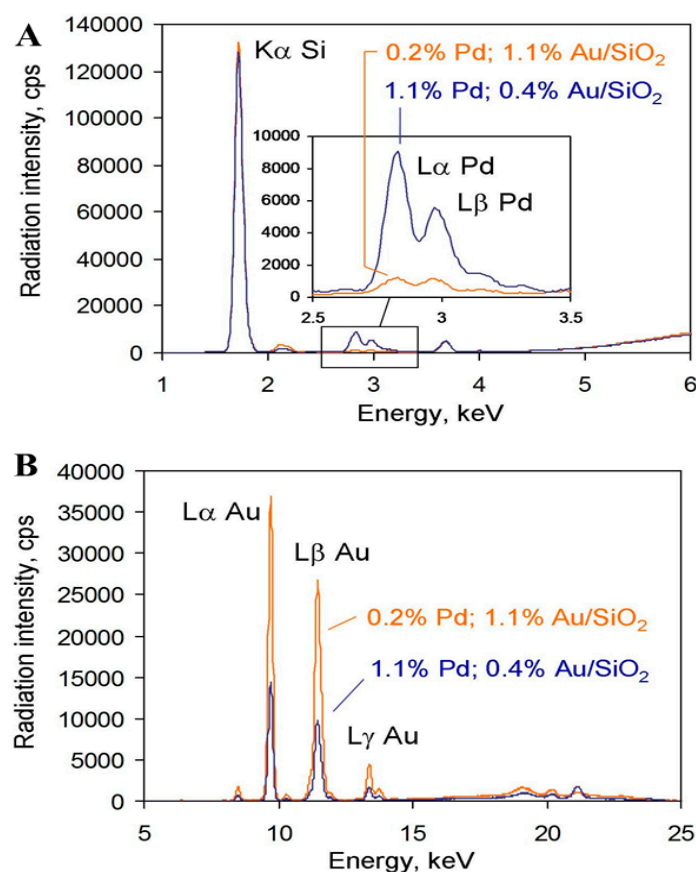


Figure 1. EDDXRF spectra of (1.1% Pd; 0.4% Au)/SiO₂ and (0.2% Pd; 1.1% Au)/SiO₂. Measurement conditions: (A) 12 kV, 750 μ A, 50 μ m Al primary beam filter, 300 s counting time, helium; (B) 30 kV, 300 μ A, 100 μ m Ag primary beam filter, 120 s counting time, air.

Table 1. The real values of Au loading in the resulting catalysts as confirmed by EDXRF and XPS analyses.

Catalyst	EDXRF (wt.%)		XPS (wt.%)		
	Pd	Au	Pd	Au	
1	0.1% Au/SiO ₂	-	0.092 \pm 0.0018	-	0.09 \pm 0.02
2	0.7% Au/SiO ₂	-	0.711 \pm 0.042	-	1.64 \pm 0.3
3	0.2% Au/C	-	0.21 \pm 0.013	-	3.2 \pm 0.3
4	(1.1% Pd; 0.4% Au)/SiO ₂	1.11 \pm 0.05	0.37 \pm 0.02	2.4 \pm 0.4	4.7 \pm 0.4
5	(0.2% Pd; 1.1% Au)/SiO ₂	0.15 \pm 0.01	1.08 \pm 0.07	1.9 \pm 0.4	4.6 \pm 0.4

For lower Au concentrations both EDXRF or XPS provide similar results which are comparable with the designed values of the Au load (Table 1, entry 1). In turn for the higher Au loads (Table 1, entries 2–5) XPS always indicated higher Au content than EDXRF. This result can be explained if we realized that X-rays (EDXRF) have a much larger penetration range compared to XPS which focuses only on the surface area. Accordingly, EDXRF relates to the bulk proportion while XPS—to the surface ratio. The surface and bulk metal to SiO₂ ratios can take the same values only for the small amounts

of the metal, when the surface portion of SiO₂ enveloped by the metal can be neglected. Otherwise, both ratios will take a different value. The higher the percentage of the metal the higher also is the surface fraction occupied by the metal and the higher the difference between the bulk and the surface concentrations and therefore between the XPS and EDXRF analyses. The comparison of the results for pure Au and its mixtures with Pd (Table 1, entry 2 vs. entries 4 and 5) indicates that this effect is specific for each metal and/or bimetallic mixture. As the weight percentage corresponds to the bulk ratio, EDXRF correlates much better with the designed metal load. To additionally prove the above-mentioned hypothesis, we performed the Atomic Absorption Spectrometry (ASA) analyses of the 0.1% and 0.7% samples. The obtained results were 0.11 ± 0.0071 wt.% for 0.1% Au/SiO₂ and 0.695 ± 0.0495 wt.% for 0.7% Au/SiO₂, which compares very well with the EDXRF results. Interestingly, the only catalyst for which we obtained the same weight percentage of Au by the XPS and EDXRF analyses is the 0.1% Au/SiO₂ system. It is also this system where Au should remain well distributed, located in the large distances between individual Au clusters. Accordingly, this should also be an optimal catalyst structure.

The XRD results of the nanogold catalysts are presented in Figure 2, which shows the X-ray diffraction patterns of the 0.7% Au/SiO₂, 0.1% Au/SiO₂, (1.1% Au; 0.4% Pd)/SiO₂, and (0.2% Pd; 1.1% Au)/SiO₂ catalysts in the range of the 2 θ angle from 10 to 120 degrees. It clearly shows the diffraction lines that correspond to the pure face-centered cubic (Fm3m) phase of Au NPs (JCPDS 01-089-3697), while the considerably weaker lines of the cubic (Fm3m) phase of Pd NPs also overlaps the Au diffraction peaks. The broad peak at the low angle range is due to the silica. The Scherrer equation was used to calculate the average size of the crystalline particles. Their size was estimated from the highest intensity XRD peak ($2\theta_{111} \sim 38.2^\circ$ for Au and $2\theta_{111} \sim 39.1^\circ$ for Pd NPs) and values from about 2 nm to about 10 nm were obtained. The lattice parameters (Å) of the investigated nanoparticles (calculated with the “Chekcell v.4” computer program) as well as the average crystallite dimensions (D) that were determined using the XRD method are listed in Table 2. In particular, we could observe that the 0.1% Au/SiO₂ (Table 2, entry 1) allows one to fully control the narrow range of Au NPs size at 7 nm. This complies with the previously discussed results of the EDXRF vs. XPS analyses.

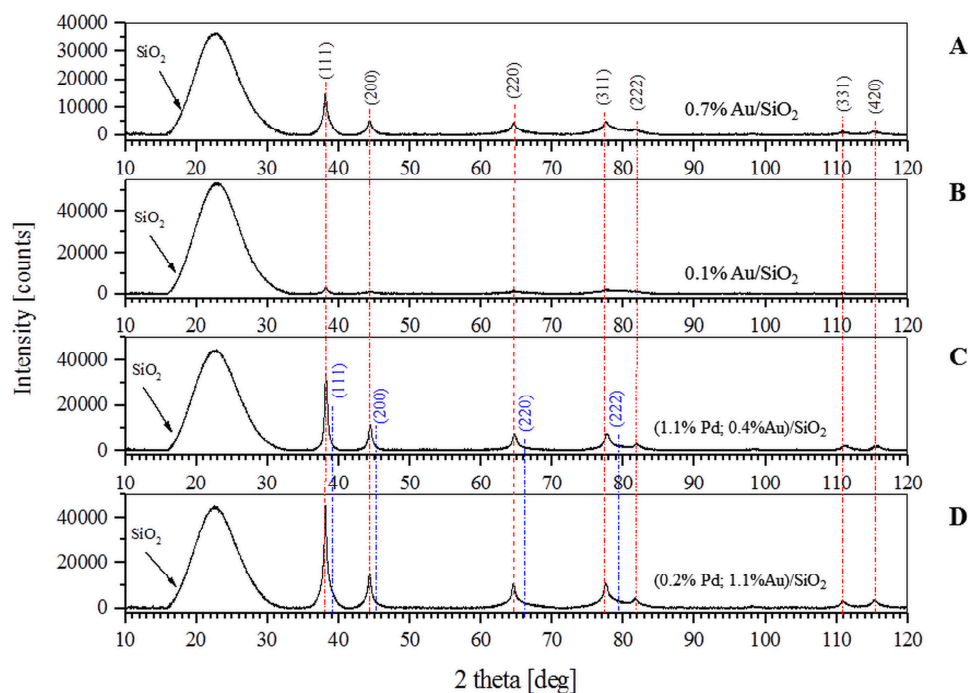


Figure 2. The X-ray diffraction patterns at 2θ : 10° – 120° for 0.7% Au/SiO₂ (A), 0.1% Au/SiO₂ (B), (1.1% Au; 0.4% Pd)/SiO₂, and (0.2% Pd; 1.1% Au)/SiO₂ (C,D) samples. Miller indices for experimental peaks of Au (black) and Pd (blue) nanoparticles are marked.

Table 2. Mean diameters (D) and lattice parameters (Å) of the nano-Au and Pd particles in the resulting catalysts as confirmed by XRD analysis.

	Catalyst	Lattice Parameters [Å]	Au and/or Pd Diameters D [nm]
1	0.1% Au/SiO ₂	a = 4.079 (±0.005)	7.0
2	0.7% Au/SiO ₂	a = 4.079 (±0.004)	2.5–8.5 ^a
3	0.2% Au/C	a = 4.080 (±0.003)	9.5
4	(1.1% Pd; 0.4% Au)/SiO ₂	for Au a = 4.074 (±0.006) for Pd a = 4.011 (±0.004)	for Au 9.0 for Pd 5.0
5	(0.2% Pd; 1.1% Au)/SiO ₂	for Au a = 4.080 (±0.007) for Pd a = 4.003 (±0.006)	for Au 2.0–10.0 ^a for Pd 5.0

^a The experimental diffraction profile is a superposition of a strong narrow peak and a less intense wide line. Both lines have the same 2θ position and different values of FWHM. The given values of Au nanoparticle size correspond to the wide and narrow lines, respectively.

The photoelectron spectra were used to derive the atomic and weight concentrations of the main elements and to obtain information about their chemical state, including potential formation about the PdAu alloy. In particular, the concentration of Au nanoparticles on SiO₂ carrier was found to be close to the values that were obtained from EDXRF (see Table 1) only for the lowest Au content. Taking into account the much lower escape depth of photoelectrons (up to 3–4 nm) than those of fluorescent photons, it concluded that there was a uniform distribution of nanoparticles on the surface of the core particles. The higher the concentrations of Au that was supported on SiO₂ and also on C the higher the difference between the XPS and EDXRF values that were determined was. This might be related to the more complete coating of the silica/carbon carriers, which leads to a reduced XPS signal from the support. The same is true for the PdAu nanoparticles. The total weight concentration was higher when it was derived from the XPS spectra. The relative intensity of the Au and Pd photoemission lines permitted some conclusions to be drawn about the core–shell structure of the mixed nanoparticles. Both samples showed a similar Pd–Au weight ratio of about 1:2 and an atomic concentration close to 1:1. This may be connected to the formation of an ordered PdAu alloy mainly on the surface of the nanoparticles. The formation of such an alloy is well recognized [16,17].

A fitting of the Au 4f photoemission lines (Figure 3) confirmed the formation of the Au chemical state with a relatively low binding energy of about 83.4 eV. A similar energy level was reported for alloyed PdAu nanoparticles [17]. The analysis of the oxidation state of Pd is difficult because the most pronounced photoemission line—Pd 3d is overlapping with the stronger Au 4d one. Thus, we performed such analysis for the Pd 4p line which is relatively weak and their behavior in various chemical states is almost not present in the literature. However, we were able to fit the spectra and for both sample containing Pd we found at least two chemical states separated by a few eV. The low binding energy doublet can be assigned to PdAu alloy while the higher energy one to oxidized Pd, which is probably PdO but higher oxidation state cannot be excluded. The results of XRD (Table 2) confirmed that the alloying as the lattice constant that was derived from the Pd diffraction lines was higher than for the pure Pd for both samples, thereby indicating the formation of an alloy.

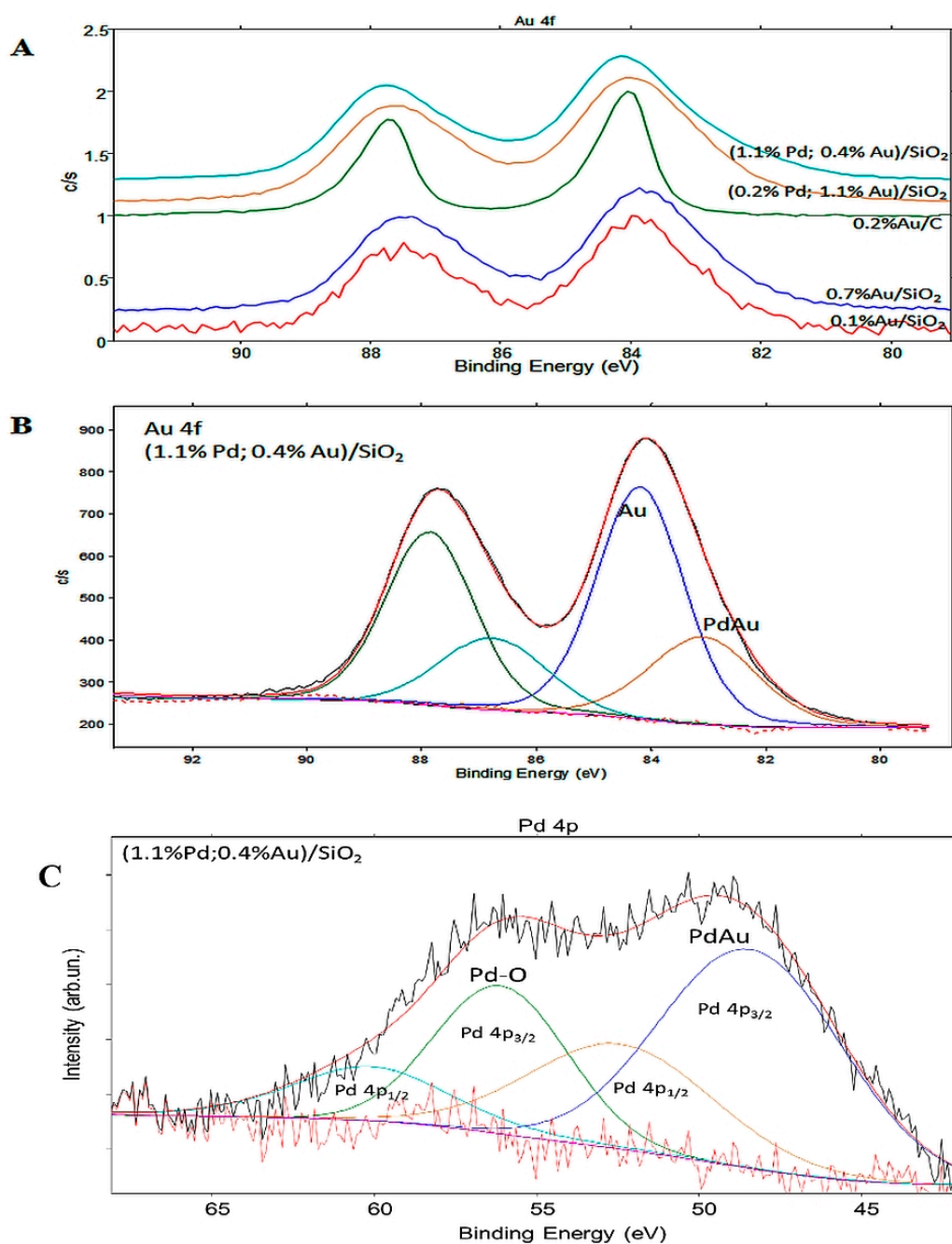


Figure 3. XPS results of the Au nanoparticles (NPs), (A) set of Au 4f spectra for the 0.1% Au/SiO₂, 0.7% Au/SiO₂, Au/C, (1.1% Pd; 0.4% Au)/SiO₂ and (0.2% Pd; 1.1% Au)/SiO₂ samples, (B) XPS spectrum and the result of fitting the Au 4f spectrum for the (1.1% Pd; 0.4% Au)/SiO₂ sample showing the two chemical states of the Au (C) Pd 4p spectrum with the result of fitting and suggested Pd chemical states for (1.1% Pd; 0.4% Au)/SiO₂.

In the (1.1% Pd; 0.4% Au)/SiO₂, the metallic nanoparticles that were distributed on the surface of SiO₂ particles were arranged individually or as conglomerates (Figure 4a–c). The Au and Pd have the same structure (space group 227), a similar atomic radius, and their lattice parameters differed only slightly. Therefore, they created particles of solid solutions. The size of the particles had a lognormal distribution with the average particle dimensions of approximately 17 nm (Figure 4d,e). In the 0.1% Au/SiO₂ catalyst, the gold nanoparticles were not heterogeneously distributed on the surface of the

SiO₂ particles. The particles were smaller and their size distribution could also be described using a lognormal distribution with the average particle dimensions of approximately 7 nm (Figure 4f).

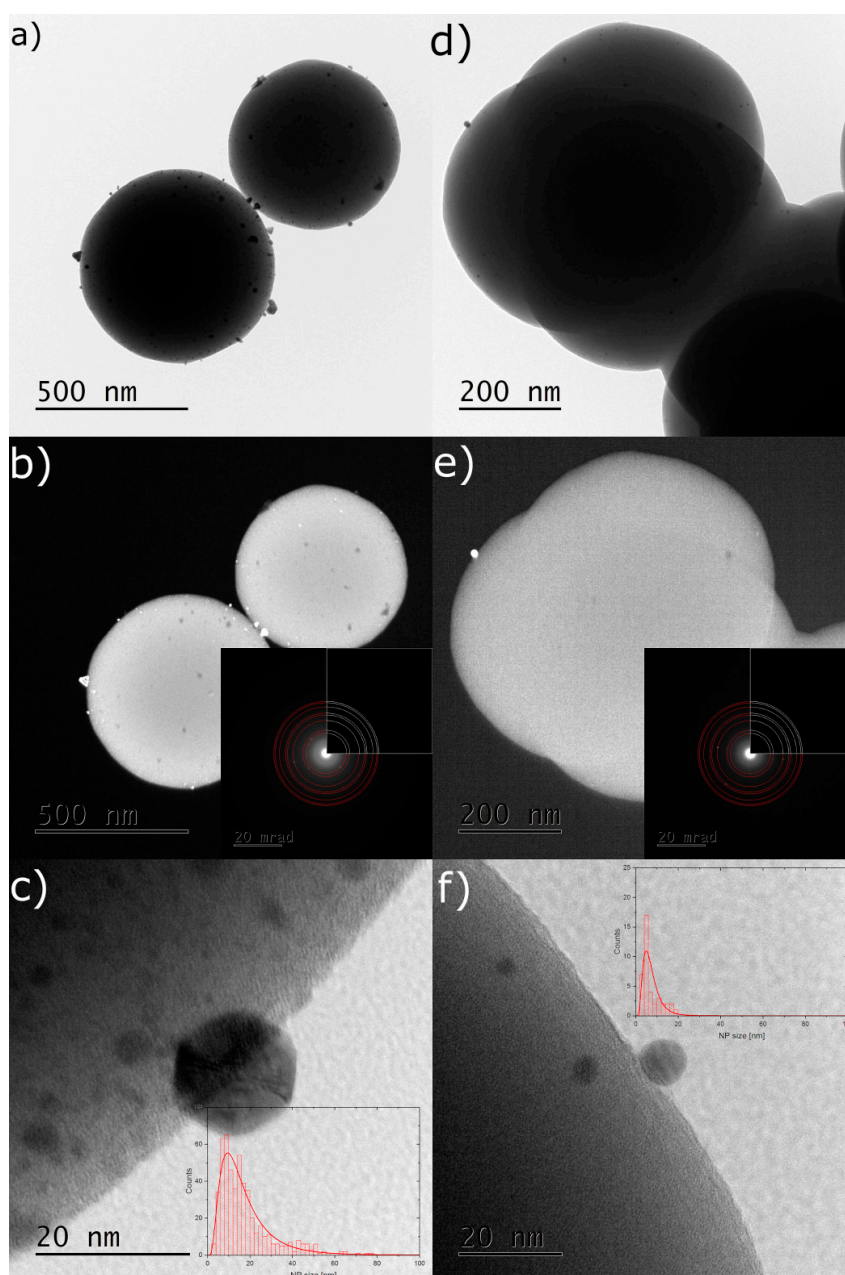


Figure 4. Representative TEM images of the (1.1% Pd; 0.4% Au)/SiO₂ (a–c) and 0.1% Au/SiO₂ (d–f) catalysts. (a,d) nanoparticles on the surface of the SiO₂ particles in the bright field image, (b,e) dark field image with an inset of the recorded selected area electron diffraction patterns overlaid by the theoretical diffraction rings for Au, (c,f) High-resolution TEM image of the nanoparticles on the SiO₂ surface with an inset showing nanoparticle size distribution.

3.2. Design and Structure of the Catalysts

When considering the carrier for nanogold dispersions, SiO₂ and C were selected as the support for the samples of the model catalysts. The catalytic feasibility of SiO₂ or C as a nanogold support have already been investigated in some oxidation reactions [18,19]. For example, we can refer to the work of Kapkowski et al. [18] on the efficiency of Au/SiO₂ catalysts in glycerol oxidation using H₂O₂/H₂O as a “clean” oxidant. Another good example might be the work of Carretin et al. [19]

on the superior catalytic properties of a 1% wt. Au/graphite catalyst in glycerol oxidation under mild reaction conditions (60 °C, 3 h, water as the solvent). Advantageously, the alcohol oxidation in the case of both of the studies that are cited proceeded under environmentally friendly conditions. However, the application of the reported catalytic systems was limited to certain types of alcohols. Here, in contrast to the literature examples, the studies on the catalytic feasibility of the resulting nano-dispersions were extended to a broader range of alcohols.

As to the different levels of Au-loading in the resulting samples, 0.1%, 0.7% and 1.2% wt. were the nominal values. The actual values of Au-loading as measured using EDXRF analysis were consistent with the nominal ones (Table 1 vs. Table S1). In an attempt to modify the catalytic properties by the formation of bimetallic active sites, a nano-Pd was selected as the second metal to enrich the active phase of the catalysts. It was assumed that synergistic interactions at the bimetallic active sites Au–Pd might lead to an increase in catalytic activity and stability in alcohol oxidation.

The TEM, SEM, XPS, and XRD analytical techniques were used to characterize the structure, dimensions and texture properties of the synthesized catalysts. The mean particle size of the nanometals in the active phase of the resulting catalysts was estimated by an XRD measurement (Table 2). The results proved that the mean particle size and distribution of the particle size of the resulting Au nanodispersions varied depending on the level of metal loading (Table 2, e.g., 0.1% Au/SiO₂ vs. 0.7% Au/SiO₂), the type of material of the support (Table 2, e.g., 0.1% Au/SiO₂ vs. 0.2% Au/C), and the co-presence of a second metallic active phase (Table 1, e.g., (1.1% Pd; 0.4% Au)/SiO₂ vs. (0.1% Pd; 1.1% Au)/SiO₂ vs. 0.7% Au/SiO₂). In all of the samples, the mean Au particle size did not exceed the critical value of 10 nm (Entries 1–5 in Table 2), which is regarded as being crucial in terms of the catalytic activity of Au. According to the literature, supported Au nanoparticles less than 10 nm in size, especially those ca. 5 nm, are typically required for catalysis [20]. It is worth noting that the resulting samples predominantly exhibited a narrow size distribution with the exception of samples 0.7% Au/SiO₂ and (0.2% Pd; 1.1% Au)/SiO₂ (Entries 2 and 6 in Table 2). The observed deviation from the narrow size distribution might be ascribed to a partial sintering of the Au nanoparticles for the samples that had a high level of Au-loading on the SiO₂ support.

The model oxidation reactions of alcohols in the presence of the resulting catalysts (Tables 3 and 4) were performed using aqueous hydrogen peroxide as the oxidant under solvent-free and base-free conditions in order to test the catalytic activity in a sustainable and environmentally benign system. When selecting the model alcohols, the criterion that the chemical reactivity of alcohols could be controlled by changing chemical structure was taken into account. Namely, a reactivity of aliphatic alcohols significantly increases in benzylic position [21]. Therefore, representatives of unactivated alcohols, namely 1-propanol and 1,2-propanediol, were used as the model alcohols in order to examine the catalytic capability for substrates that are more resistant to oxidation. A comparative evaluation of the catalytic performance was carried out taking into account the values of turnover number, turnover frequency, reaction conversion, selectivity, and yield of the main products that were obtained (Tables 3 and 4). These parameters varied depending on the catalyst forms. The results clearly proved that using the catalytic properties of 0.1% Au/SiO₂ to activate the conversion of the alcohols were considerably greater compared to the other catalysts (Entry 1 vs. entries 2–5 in Tables 3 and 4). The catalytic system of 0.1% Au/SiO₂ afforded the highest conversion of ca. 77% and 100% for the oxidation of 1-propanol and 1,2-propanediol, respectively (Entry 1 in Tables 3 and 4). Compared to the blank sample and the pure unsupported carriers (used as blind samples), the selectivity of the investigated reaction obviously prefers the formation of the products of oxygenation more than a direct carbonyl product, e.g., formic acid or propionic acid in 1-propanol oxidation instead direct propanol (Table 3 entries 1 vs. 6 and 7). In addition, among the catalysts that were tested, 0.1% Au/SiO₂ had notably higher values of the turnover number (TON) and turnover frequency (TOF) (Entry 1 vs. entries 2–5 in Tables 3 and 4). The large discrepancy in the TON or TOF values between 0.1% Au/SiO₂ and the other catalysts confirmed that 0.1% Au/SiO₂ exhibited the highest catalytic efficiency among the samples that were analyzed. The selectivity of the 0.1% Au/SiO₂ system varied depending on the structure of

the substrate. In particular, the catalytic oxidation of 1-propanol over 0.1% Au/SiO₂ into acetic acid afforded a moderate selectivity ca. 57% (Entry 1 in Table 3), while the oxidation of 1,2-propanediol in the presence of 0.1% Au/SiO₂ resulted in a high selectivity of acetic acid ca. 95% (Entry 1 in Table 4).

Table 3. Catalytic performance of the resulting catalysts in the oxidation of 1-propanol into acetic acid under reaction conditions as described in Experiment 2.3.

	Catalyst ^a	α^b (%)	TON ^c	TOF ^d (h ⁻¹)	Selectivity (%)				Yield AA (%)
					FA	AA	PA	OS	
1	0.1% Au/SiO ₂	76.6	3774	189	2.4	56.7	18.3	22.6	43.4
2	0.7% Au/SiO ₂	4.8	34	2	0	70	0	30	3.4
3	0.2% Au/C	43.5	1071	54	0	19	51.9	29.1	8.3
4	(0.2% Pd; 1.1% Au)/SiO ₂	18.0	525	26	0	100	0	0	18
5	(1.1% Pd; 0.4% Au)/SiO ₂	3.2	36	2	0	19.9	0	79.9	0.6
6	None	96.7	0	0	16.1	0	17.4	66.5	0
7	SiO ₂	47.1	0	0	13.5	2.2	39.3	45	1.1
8	C	95.8	0	0	39.1	1.9	21.6	37.5	1.8

^a 0.3 mol/L of 1-propanol in the reaction mixture (1-propanol/H₂O₂ molar ratio 1:20), 20 mg of the catalyst (0.1–1.9 μ mol Au), 85 °C, 20 h, 300 rpm. ^b α : system conversion degree. ^c Turnover number (TON). ^d Turnover frequency (TOF) based on the total nanometal content in the material. FA: formic acid, AA: acetic acid, PA: propionic acid, OS: others.

Table 4. Catalytic performance of the resulting catalysts in the oxidation of 1,2-propanediol into acetic acid under reaction conditions as described in Experiment 2.3.

	Catalyst ^a	α^b (%)	TON ^c	TOF ^d (h ⁻¹)	Selectivity ^d (%)					Yield AA (%)
					FA	AA	ACNE	HYNE	OS	
1	0.1% Au/SiO ₂	100	4924	246	1.7	94.8	1.3	0	2.2	94.8
2	0.7% Au/SiO ₂	3.8	27	2	0	0	25	75	28.6	0
3	0.2% Au/C	28.5	702	35	0	52.5	7.5	37.5	2.5	15.0
4	(1.1% Pd; 0.4% Au)/SiO ₂	3.8	56	3	0	0	50	50	0	0
5	(0.2% Pd; 1.1% Au)/SiO ₂	1.5	27	1	0	0	0	33.3	66.7	0
6	None	84.7	0	0	18.5	75.5	0.8	2.2	3.0	63.9
7	SiO ₂	90.1	0	0	29.7	67.6	0.3	1.4	1.0	60.9
8	C	17.4	0	0	28.6	30.0	1.0	38.7	1.7	5.2

^a 0.3 mol/L of 1,2-propanediol in the reaction mixture (1,2-propanediol/H₂O₂ molar ratio 1:20), 20 mg of the catalyst (0.1–1.9 μ mol Au), 85 °C, 20 h, 300 rpm. ^b α : system conversion degree. ^c Turnover number (TON). ^d Turnover frequency (TOF) based on the total nanometal content in the material. FA: formic acid, AA: acetic acid, ACNE: acetone, HYNE: 1-hydroxyacetone, OS: others.

The analysis of the data from Tables 2–4 offered insight on how the structure of the catalysts might affect the catalytic performance. For instance, the results confirmed that the catalytic performance of the Au/SiO₂ system was strongly affected by the level of Au-loading. As was mentioned previously, the 0.1% Au/SiO₂ catalyst had the highest degree of conversions among the catalysts that were used (Entry 1 in Tables 3 and 4). Surprisingly, however, increasing the level of Au loading from 0.1% to 0.7% wt. for the Au/SiO₂ system caused a dramatic decline in the degree of conversions (Entry 2 in Tables 3 and 4). The oxidation over the 0.7% Au/SiO₂ catalyst resulted in poor conversions of ca. 5% and 7% for the reactions with 1-propanol and 1,2-propanediol, respectively. Furthermore, an analysis of the data from Tables 2–4 suggests that the catalytic activity of the Au dispersions may be sensitive to the particle size of the nano-Au as well as their size distribution. In this context, the particle size of nanometals for dispersions such as 0.7% Au/SiO₂ or (0.2% Pd; 1.1% Au)/SiO₂ (Entries 2 and 5 in Table 2) appeared to be insufficient to facilitate alcohol conversions (Entries 2 and 5 in Tables 3 and 4). A further analysis of the data from Table 2 suggested that the particle size of the active phase might be affected by changes in the level of Au-loading. In this respect, a higher level of Au-loading could result in the partial sintering of the Au-particles, and subsequently could lead to a wide size distribution of the Au particles as was observed for the 0.7% Au/SiO₂ or (0.2% Pd; 1.1% Au)/SiO₂ (Entries 2 and 5 in Table 2). This phenomenon might also contribute to the worsening of the catalytic performance of the resulting samples. It is worth mentioning that the 0.1% Au/SiO₂ catalyst appeared optimal, as

expected from the EDXRF and XPS analyses. A possible reason for the deactivation of similar systems of AuPd alloys was ascribed by Hutchings et al. for the high Au-to-Pd ratio alloys which are especially sensitive to the high reaction temperature [22]. The results that were obtained also confirmed that the catalytic performance of the catalysts might be affected by the type of support, i.e., replacing the SiO₂ support with a C support for the catalysts with a 0.2% wt. Au loading afforded higher conversion values and resulted in a moderate improvement of the catalytic efficiency (Entry 2 in Tables 3 and 4 vs. Entry 3 in Tables 3 and 4). In this context, better wettability of polar silica carrier by polar reagents can explain the difference between the SiO₂ vs. C carrier. Moreover, the results presented in Tables 3 and 4 indicate that oxidation depends upon many factors. In particular, paradoxically the highest conversion is observed either for the 0.1% Au/SiO₂ or for the non-catalytic or SiO₂ catalyzed reaction. However, it is only the catalytic 0.1% Au/SiO₂ system where the conversion and selectivity are high enough, e.g., this can reach as much as ca. 95% AA for 1,2-propanediol (Table 4, entry 1). The individual values for 1-propanol (Table 3) or 1,2-propanediol (Table 4) compares as follows: (0.1% Au/SiO₂ ca. 77%: Table 3, entry 1; 100%: Table 4, entry 1) vs. (none catalyst ca. 47%: Table 3, entry 7; 90%: Table 4, entry 7) vs. (none catalyst ca. 97%: Table 3, entry 6; 85%: Table 4, entry 6). To explain this effect, we should understand that the Au NPs catalyze not only the oxidation of alcohol but also the decomposition of H₂O₂. The latter effect is especially visible at higher temperatures. Therefore, an increasing temperature, from one side, enhances the reaction but, from the other side, enhances also the decomposition of the oxidant. In this context our previous experiments showed that 85 °C appeared more or less optimal for the process. In turn, in the non-catalytic or SiO₂ catalyzed systems the decomposition of H₂O₂ is much slower, therefore, the conversion at high temperature can be still high; however, the selectivity of the reaction is much lower and the reaction yields a variety of products. As the importance of the decomposition of H₂O₂ increases with the increase of the metal load, therefore, also the conversions are lower when Au load increases.

The studies also enabled an examination into whether the presence of bimetallic sites in the active phase of (1.1% Pd; 0.4% Au)/SiO₂ and (0.2% Pd; 1.1% Au)/SiO₂ enhanced the catalytic performance. However, the conjugation of Au and Pd appeared to be less important than was expected. Although this did not afford a significant improvement of the alcohol conversions (Entries 4 and 5 in Tables 3 and 4), a synergistic effect could be observed for 1-propanol at (0.2% Pd; 1.1% Au)/SiO₂ where the selectivity of the acetic acid formation amounted to 100% compared to the other catalysts (Entry 4 vs. entries 1–3 and 5 in Table 3). On the other hand, the selectivity of oxidation of 1-propanol to acetic acid at the (1.1%Pd; 0.4% Au)/SiO₂ catalyst was lower (ca. 20%), when the formation of other byproducts was promoted with the highest selectivity of ca. 79.9% compared to the other catalytic systems (Entry 5 vs. entries 1–4 in Table 3). Another example of the synergic effect between Au and the Pd alloy is that the selectivity of the formation of acetone (ca. 50%) and 1-hydroxyacetone (ca. 50%) was enhanced while the oxidation of 1,2-propanediol at (1.1% Pd; 0.4% Au)/SiO₂ compared to the other catalytic systems (Entry 4 vs. entries 1–3 and 6 in Table 4).

From the above comparative analyses, it can be concluded that 0.1% Au/SiO₂ had the most advantageous catalytic performance and appeared to be the most potent catalyst among the resulting samples. Therefore, 0.1% Au/SiO₂ was selected for further studies whose aim was to examine its catalytic utility in the oxidation of a broader spectrum of alcohols. In order to investigate the scope of alcohol oxidation with the 0.1% Au/SiO₂–H₂O₂ system, the studies were extended to various structurally different alcohols. The reactions were carried out under the same experimental conditions as was the case of the previous model reactions. The results of this part of the studies are summarized in Table 5, which covers the main products of the oxidation of the alcohols. The formation of acetic acid was specifically monitored as this product could have been formed in all of the cases. The highest oxidation yields to acetic acid were observed for the dihydric alcohols, i.e., 1,2-propanediol of ca. 94.8% and 2,3-butanediol, ca. 57.6% (Entries 6 and 8 in Table 5). For the oxidation of the monoalcohols, the highest acetic acid yields were observed for 1-propanol and 2-propanol at 43.4% and 51.7%, respectively (Entries 2 and 3 in Table 5). The low nanogold content and good wettability of the carrier by polar

reagents enabled the efficient use of hydrogen peroxide, thus promoting the formation of organic acids. It should also be remembered that the values of the conversion, selectivity, and yield of acetic acid and other products that were obtained varied from moderate to high depending on the alcohol substrate (Entries 1–6 in Table 5). The results confirmed that under mild reaction conditions, the 0.1% Au/SiO₂-H₂O₂ system can effectively facilitate the catalytic oxidation of various nonactivated alcohols, including the most inactive primary aliphatic alcohols.

Table 5. Summary of the catalytic oxidation of various structurally different monohydric and dihydric aliphatic alcohols into acetic acid in the presence of the 0.1% Au/SiO₂ catalyst under reaction conditions as described in Section 2.3.

	Aliphatic Alcohol ^a	α (%) ^b	TON ^c	TOF ^d (h ⁻¹)	Selectivity (%)			Yield AA (%)
					OMP	AA	OS	
1	ethanol	47.3	2329	116	11.2 ^e	51.3	37.5	24.3
2	1-propanol	76.6	3774	189	18.3 ^f	56.7	25	43.4
3	2-propanol	97.8	4816	241	40.5 ^g	52.9	6.6	51.7
4	2-butanol	29.4	1448	72	19.2 ^h	44.8	36	13.2
5	1,2-ethanediol	50.6	2492	125	46.9 ⁱ	1.2	51.9	0.6
6	1,2-propanediol	100	4924	246	1.7 ⁱ	94.8	3.5	94.8
7	1,3-propanediol	94.0	4629	231	45.6 ^j	28.7	25.7	27
8	2,3-butanediol	68.3	3363	168	6.1 ^e	84.3	9.6	57.6

^a 0.3 mol/L of aliphatic alcohol in the reaction mixture (aliphatic alcohol/H₂O₂ molar ratio 1:20), 20 mg of the catalyst (0.1 μ mol Au), 85 °C, 20 h, 300 rpm. ^b α : system conversion degree. ^c Turnover number (TON) refers to the total Au content in the catalyst. ^d Turnover frequency (TOF) refers to the total Au content in the catalyst. OMP: other main products of the oxidation of alcohols: ^e acetaldehyde, ^f propionic acid, ^g acetone, ^h 2-butanone, ⁱ formic acid, ^j 3-hydroxypropanoic acid, AA: acetic acid, OS: other products.

In Figure 5 we illustrated the conversion and selectivity of oxidation as a function of the ratio of 1,2-propanediol to H₂O₂ for 0.1% Au/SiO₂. Milder oxidation conditions helped, to a limited extent, to avoid deep oxidative decomposition of the reactants to AA or FA acids. The possible reaction mechanism can involve two complementary routes (Scheme 1). First one comprises the C–C bond cleavage in 1,2-propanediol yielding formaldehyde and acetaldehyde (ACDE), which are further oxidized to the corresponding acids (AA or FA). In turn, a second route involves (oxy)dehydrogenation to hydroxyacetone (HYNE) and acetone (ACNE). In the last stage of oxidation, the latter two C₃ products are oxidized to acetic acid (AA) and formic acid (FA). For the concentration of propylene glycol to H₂O₂/H₂O of 1:1, 1:3, and 1:5 we observed a high fraction of C₃ products (HYNE and ACNE), respectively. The increasing concentration of oxidant (10, 15, and 20 moles) enhanced the oxidative degradation of this reactants. For the concentration of 1:20 AA was the only product in the reaction mixture, because FA was oxidized to CO₂. Nanogold has been extensively studied as a catalyst for glycerol, propane-1,2-diol, n-alkyl alcohol oxidation in the presence of Brønsted bases or base free conditions using oxygen and peroxides as oxidants [23–25]. The Au/SiO₂ system appeared also an efficient catalyst in oxidation of cyclohexene or D-glucose [26]. Della Pina et al. described oxidation of 1,2-propanediol at 0.5% Au/TiO₂ and 1.0% AuPd/TiO₂ with O₂ to lactate with acetate and formate as byproducts (conversion up to 95%). Also, benzyl alcohol can be oxidized by H₂O₂ in the presence of Au nanoparticles (1 nm) deposited at SBA-15 silica carrier with 96% conversion which yielded benzylic acid as a main product [23]. Dimitratos et al. obtained benzylic acid at the Au/SBA-15 catalyst suspended in the water/K₂CO₃ system with 96% conversion degree and 87% selectivity. In turn, the Au/C system used in catalytic oxidation of glycerol, propylene or ethylene glycol in water/sodium hydroxide yielded acidic products [24,25]. These were also the main products of our reactions (Table 5). Moreover, the conversion and selectivity to AA could be high (Figure 5). Although the oxidation of C₃ alcohols to AA may seem unattractive, AA is an important reagent and intermediate and solvent from the industrial point of view.

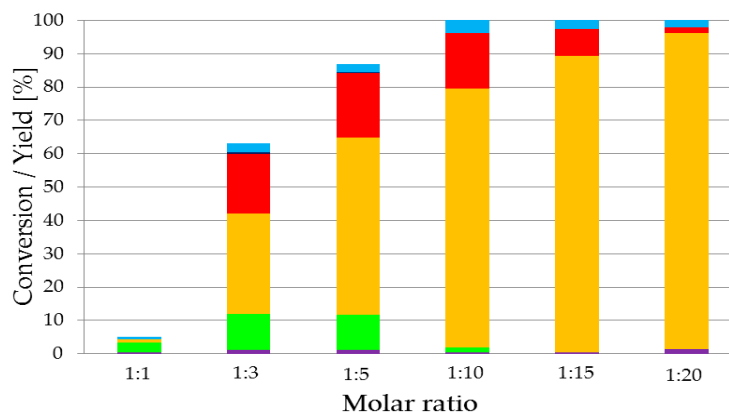
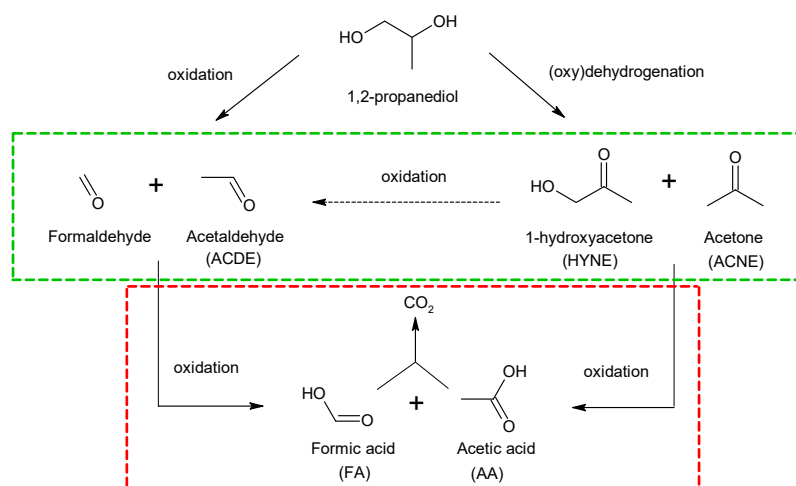


Figure 5. The yields of individual products and total conversion for the reaction of 1 mol/L 1,2-propanediol and 30% H₂O₂/H₂O. Reaction conditions: 20 mg 0.1% Au/SiO₂, 85 °C, 20 h, 200 rpm, 0.3 mol/L concentration 1,2-propanediol in reaction mixture after mixing the reagents. Particular colors at chart refer to: ■ acetone (ACNE), ■ 1-hydroxyacetone (HYNE), ■ acetic acid (AA), ■ formic acid (FA), ■ acetaldehyde (ACDE) ■ other products (OS). The experiments were conducted for the same volume of reagents (0.5 mL alcohol with 1.0 mL H₂O₂/H₂O solution with increasing molar ratio of oxidant) in procedure described in Section 2.3.



Scheme 1. Two route mechanism of oxidation or (oxy)dehydrogenation of 1,2-propanediol to acetic acid. Products in the green frame were mostly observed for the reaction mixture of 1,2-propanediol to H₂O₂ in the proportion of 1:1, 1:3, or 1:5. Products in the red frame were mostly observed for the reaction mixture of 1,2-propanediol to H₂O₂ in the proportion of 1:10, 1:15 or 1:20. The legend sitting under chemical formulas refers to the acronyms used in then text.

The search for an efficient, versatile, and green system for the oxidation of alcohols remains a significant challenge [27]. In view of presented results, the 0.1% Au/SiO₂ catalyst seems to have prospects for wide applications for alcohol oxidation, and notably, SiO₂ appears to be a promising support material for nanogold particles. This is an intriguing finding taking into account the recent trends in the investigation for an optimal material for nano-Au support, which is one use of reducible metal oxides, usually Fe₃O₄, ZnO, CeO₂, and TiO₂ [28]. In fact, the interactions between the active phase and active support (e.g., Au-TiO₂, Au-Fe₃O₄) via the formation of oxygen vacancies in reducible metal oxides are recognized as being one of the most effective ways to enhance the catalytic properties [29]. By contrast, SiO₂ is a representative of the non-reducible metal oxides, which are regarded as being relatively inert materials for nano-Au support [30]. In contrast to Au/TiO₂, which has been discussed in the most detail, Au/SiO₂ has been minimally studied primarily due to the low activity of SiO₂ and the difficulties in preparing catalysts [30,31]. The typical deposition method

of Au on SiO₂ might pose a problem due to the low point of the zero charge of SiO₂ [31]; however; we have previously showed the performance of such catalysts [15]. The utility of SiO₂ as a support for Au can be beneficial from the practical point of view and seems to provide some advantages over the reducible metal oxides. First of all, SiO₂ has a greatly developed specific surface area that has a high porosity, which, in turn, can favor good dispersions of Au nanoparticles [32]. By contrast, TiO₂ features a low surface area, especially after calcination, and requires further modifications to facilitate Au dispersion [33]. Most importantly, the results of our study have proven that the deposition of Au on SiO₂ with a level of Au loading as low as 0.1% wt. led to an efficient catalytic system for the oxidation of a broad spectrum of alcohols under mild reaction conditions. To the best of our knowledge, this result is being reported for the first time. Of course, the pioneering studies of Cao's group [34] provided proof that 1% wt. Au/TiO₂-H₂O₂ was a highly effective system in Cao et al.'s [34] procedure; however; this means that the Au loading was ten times higher than the level of Au that was needed in the Au/SiO₂-H₂O₂ system that is reported here. The additional advantage of SiO₂ as the material for Au support is its relatively low price and higher chemical stability [35] compared to other materials such as TiO₂. As to its catalytic stability, the commercially available Au/TiO₂ tends to deteriorate during storage as it is both light- and moisture-sensitive [36]. The study of Sárkány on acetylene hydrogenation [37] demonstrated that the deactivation of Au/TiO₂ proceeded faster than in the case Au/SiO₂. In the studies of Masoud et al. on the selective hydrogenation of butadiene [38], the Au/SiO₂ catalysts clearly outperformed the Au/TiO₂ catalysts after a certain time-on-stream. In addition, SiO₂ is generally recognized as being safe by the FDA [39,40], whereas TiO₂ exhibits some level of toxicity [41]. This is an important advantage of using Au/SiO₂ as a catalyst, especially in the case alcohol oxidation for pharmaceutical syntheses.

As the fine chemical industry moves toward green and sustainable chemistry, the proposed 0.1% Au/SiO₂-H₂O₂ system could be a prospective approach towards the development of an efficient catalytic nanogold platform for the oxidation of a broad spectrum of alcohols.

4. Conclusions

The presented results proved that the 0.1% Au/SiO₂ catalyst has a good potential for the environmentally benign oxidation of alcohols with H₂O₂ in the absence of a base under organic solvent-free conditions. Notably, the 0.1% Au/SiO₂ system exhibits sufficient activity for the oxidation of various structurally different alcohols, including those that are resistant to oxidation—primary aliphatic alcohols. At the same time under acidic conditions the Au/SiO₂ catalyst which is unstable in the basic conditions, shows much higher durability. The paradoxical effect of the higher activity of the catalyst of the low Au load on the silica surface is also worth mentioning. In this context the catalyst quality can be monitored by the comparison of the EDXRF vs. XPS analyses.

Supplementary Materials: The following are available online at <http://www.mdpi.com/2079-4991/9/3/442/s1>, Table S1: The amount of the precursor (g) per 100 g of tetraethyl orthosilicate that was required for the syntheses of the catalysts in Experiment 2.1.1, Figure S1: The ¹H NMR (A), ¹³C NMR (B), COSY (C), HMQC (D) spectra of the crude reaction mixture for the catalytic oxidation of 2-propanol in the presence of 0.1% Au/SiO₂ under the reaction conditions as described in Experiment 2.3., Figure S2: The ¹H NMR (A), ¹³C NMR (B), COSY (C), HMQC (D) spectra of the crude reaction mixture for the oxidation of 1,3-propanediol in the presence of 0.1% Au/SiO₂ under the reaction conditions as described in Experiment 2.3.

Author Contributions: Conceptualization, J.P., M.K., and A.N.-W.; methodology, M.P.B. and K.G.; formal analysis, J.P., M.K., and A.N.-W.; investigation, M.K., P.B., R.S., M.Z., J.S., J.K., and K.B.; writing—original draft preparation, J.P., A.N.-W., M.K., P.B., R.S., M.Z., J.S., J.K., and K.B.; writing—review and editing, J.P., A.N.-W., and M.K.; visualization, M.K.; project administration, J.P.; funding acquisition, J.P.

Funding: This work was supported by The National Centre for Research and Development (grants: TANGO1 No. TANGO1/266384/NCBR/2015 and ORGANOMET No. PBS2/A5/40/2014) and National Science Centre (grant MINIATURA2 No. DEC-2018/02/X/ST5/00450).

Acknowledgments: Maciej Kapkowski is grateful for the support of the Mobilność kadry programme no. WMFCh.306.2018. The authors would like to express their appreciation for the technical assistance of Kamila Czerna and Judyta Popiel.

Conflicts of Interest: The authors declare no conflict of interest. The funders had no role in the design of the study; in the collection, analyses, or interpretation of data; in the writing of the manuscript, or in the decision to publish the results.

References

1. Sheldon, R.A.; Arends, I.W.C.E.; Hanefeld, U. *Green Chemistry and Catalysis*, 1st ed.; Wiley-VCH Verlag GmbH & Co. KGaA: Weinheim, Germany, 2007; pp. 170–183.
2. Tojo, G.; Fernandez, M.I. *Oxidation of Alcohols to Aldehydes and Ketones—A Guide to Current Practice*, 1st ed.; Springer Science & Business Media, Inc.: New York, NY, USA, 2006; pp. 1, 289, 331, 339.
3. Sheldon, R.A. Recent advances in green catalytic oxidations of alcohols in aqueous media. *Catal. Today* **2015**, *247*, 4–13. [[CrossRef](#)]
4. Haruta, M.; Kobayashi, T.; Sano, H.; Yamada, N. Novel gold catalysts for the oxidation of carbon monoxide at a temperature far below 0 °C. *Chem. Lett.* **1987**, *16*, 405–408. [[CrossRef](#)]
5. Xie, X.; Li, Y.; Liu, Z.Q.; Haruta, M.; Shen, W. Low-temperature oxidation of CO catalysed by Co₃O₄ nanorods. *Nature* **2009**, *458*, 746–749. [[CrossRef](#)] [[PubMed](#)]
6. Ciriminna, R.; Falletta, E.; Della Pina, C.; Teles, J.H.; Pagliaro, M. Industrial applications of gold catalysis. *Angew. Chem., Int. Ed.* **2016**, *55*, 14210–14217. [[CrossRef](#)] [[PubMed](#)]
7. Liu, X.; He, L.; Liu, Y.M.; Cao, Y. Supported gold catalysis: From small molecule activation to green chemical synthesis. *Acc. Chem. Res.* **2014**, *47*, 793–804. [[CrossRef](#)] [[PubMed](#)]
8. Ciriminna, R.; Pandarus, V.; Delisi, R.; Scurria, A.; Casaletto, M.P.; Giordano, F.; Béland, F.; Pagliaro, M. Sol-gel encapsulation of Au nanoparticles in hybrid silica improves gold oxidation catalysis. *Chem. Cent. J.* **2016**, *10*, 2–6. [[CrossRef](#)] [[PubMed](#)]
9. Bond, G.C.; Louis, C.; Thompson, D. *Catalysis by Gold*, 1st ed.; Imperial College Press: London, UK, 2006; pp. 22–35.
10. Haruta, M. Gold as a novel catalyst in the 21st century: Preparation, working mechanism and applications. *Gold Bull.* **2004**, *37*, 27–36. [[CrossRef](#)]
11. Arends, I.W.C.E.; Sheldon, R.A. Modern oxidation of alcohols using environmentally benign oxidants. In *Modern Oxidation Methods*, 2nd ed.; Bäckvall, J.E., Ed.; Wiley-VCH Verlag GmbH & Co. KGaA: Weinheim, Germany, 2010; pp. 147–185.
12. Biffis, A.; Minati, L. Efficient aerobic oxidation of alcohols in water catalysed by microgel-stabilised metal nanoclusters. *J. Catal.* **2005**, *236*, 405–409. [[CrossRef](#)]
13. Abad, A.; Almela, C.; Corma, A.; Garcia, H. Unique gold chemoselectivity for the aerobic oxidation of allylic alcohols. *Chem. Commun.* **2006**, *0*, 3178–3180. [[CrossRef](#)] [[PubMed](#)]
14. Mäki-Arvela, P.; Murzin, D.Y. Effect of catalyst synthesis parameters on the metal particle size. *Appl. Catal., A* **2013**, *451*, 251–281. [[CrossRef](#)]
15. Korzec, M.; Bartczak, P.; Niemczyk, A.; Szade, J.; Kapkowski, M.; Zenderowska, P.; Balin, K.; Lelaćko, J.; Polanski, J. Bimetallic nano Pd/PdO/Cu system as a highly effective catalyst for the Sonogashira reaction. *J. Catal.* **2014**, *313*, 1–8. [[CrossRef](#)]
16. Ding, Y.; Fan, F.; Tian, Z.; Wang, Z.L. Atomic structure of Au-Pd bimetallic alloyed nanoparticles. *J. Am. Chem. Soc.* **2010**, *132*, 12480–12486. [[CrossRef](#)] [[PubMed](#)]
17. Lee, Y.S.; Jeon, Y.; Chung, Y.D.; Lim, K.Y.; Whang, C.N.; Oh, S.J. Charge redistribution and electronic behavior in Pd-Au alloys. *J. Korean Phys. Soc.* **2000**, *37*, 451–455.
18. Kapkowski, M.; Bartczak, P.; Korzec, M.; Sitko, R.; Szade, J.; Balin, K.; Lelaćko, J.; Polanski, J. SiO₂-, Cu-, and Ni-supported Au nanoparticles for selective glycerol oxidation in the liquid phase. *J. Catal.* **2014**, *319*, 110–118. [[CrossRef](#)]
19. Carrettin, S.; McMorn, P.; Johnston, P.; Griffin, K.; Hutchings, G.J. Selective oxidation of glycerol to glyceric acid using a gold catalyst in aqueous sodium hydroxide. *Chem. Commun.* **2002**, *0*, 696–697. [[CrossRef](#)]
20. Huang, W. Model catalysts for Au catalysis: From single crystals to supported nanoparticles. In *Heterogeneous Gold Catalysts and Catalysis*, 1st ed.; Ma, Z., Dai, S., Eds.; The Royal Society of Chemistry: Cambridge, UK, 2014; pp. 533–574.
21. Smith, M.B. *March's Advanced Organic Chemistry: Reactions, Mechanisms, and Structure*, 7th ed.; John Wiley & Sons, Inc.: New Jersey, NJ, USA, 2013; pp. 1758–1762.

22. Brett, G.L.; He, Q.; Hammond, C.; Miedziak, P.J.; Dimitratos, N.; Sankar, M.; Herzing, A.A.; Conte, M.; Lopez-Sanchez, J.A.; Kiely, C.J.; et al. Selective oxidation of glycerol by highly active bimetallic catalysts at ambient temperature under base-free conditions. *Angew. Chem. Int. Ed.* **2011**, *50*, 10136–10139. [CrossRef] [PubMed]
23. Della Pina, C.; Falletta, E.; Rossi, M. Update on selective oxidation using gold. *Chem. Soc. Rev.* **2012**, *41*, 350–369. [CrossRef] [PubMed]
24. Dimitratos, N.; Lopez-Sanchez, J.A.; Hutchings, G.J. Selective liquid phase oxidation with supported metal nanoparticles. *Chem. Sci.* **2012**, *3*, 20–44. [CrossRef]
25. Villa, A.; Dimitratos, N.; Chan-Thaw, C.E.; Hammond, C.; Prati, L.; Hutchings, G.J. Glycerol Oxidation Using Gold-Containing Catalysts. *Acc. Chem. Res.* **2015**, *48*, 1403–1412. [CrossRef] [PubMed]
26. Bujak, P.; Bartzczak, P.; Polanski, J. Highly efficient room-temperature oxidation of cyclohexene and D-glucose over nanogold Au/SiO₂ in water. *J. Catal.* **2012**, *295*, 15–21. [CrossRef]
27. Ciriminna, R.; Pandarus, V.; Béland, F.; Xu, Y.J.; Pagliaro, M. Heterogeneously catalyzed alcohol oxidation for the fine chemical industry. *Org. Process Res. Dev.* **2015**, *19*, 1554–1558. [CrossRef]
28. Liotta, L.F. New trends in gold catalysts. *Catalysts* **2014**, *4*, 299–304. [CrossRef]
29. Wu, H.; Liotta, L.F. Metal-support interaction effects on gold catalysts over reducible oxides. In *Heterogeneous Gold Catalysts and Catalysis*, 1st ed.; Ma, Z., Dai, S., Eds.; The Royal Society of Chemistry: Cambridge, UK, 2014; pp. 462–488.
30. Min, B.K.; Santra, A.K.; Goodman, D.W. Understanding silica-supported metal catalysts: Pd/silica as a case study. *Catal. Today* **2003**, *85*, 113–124. [CrossRef]
31. Corma, A.; Garcia, H. Supported gold nanoparticles as catalysts for organic reactions. *Chem. Soc. Rev.* **2008**, *37*, 2096–2126. [CrossRef] [PubMed]
32. Corma, A.; Garcia, H. Supported Gold Nanoparticles as Oxidation Catalysts. In *Nanoparticles and Catalysis*, 1st ed.; Astruc, D., Ed.; Wiley-VCH Verlag GmbH & Co. KGaA: Weinheim, Germany, 2008; pp. 389–426.
33. Zhou, L.; Chen, M.; Wang, Y.; Su, Y.; Yang, X.; Chen, C.; Xu, J. Au/mesoporous-TiO₂ as catalyst for the oxidation of alcohols to carboxylic acids with molecular oxygen in water. *Appl. Catal. A* **2014**, *475*, 347–354. [CrossRef]
34. Ni, J.; Yu, W.J.; He, L.; Sun, H.; Cao, Y.; He, H.Y.; Fan, K.N. A green and efficient oxidation of alcohols by supported gold catalysts using aqueous H₂O₂ under organic solvent-free conditions. *Green Chem.* **2009**, *11*, 756–759. [CrossRef]
35. Martínez, F.; Molina, R.; Pariente, M.I.; Siles, J.A.; Melero, J.A. Low-cost Fe/SiO₂ catalysts for continuous Fenton processes. *Catal. Today* **2017**, *280*, 176–183. [CrossRef]
36. Zanella, R.; Louis, C. Influence of the conditions of thermal treatments and of storage on the size of the gold particles in Au/TiO₂ samples. *Catal. Today* **2005**, *107–108*, 768–777. [CrossRef]
37. Sárkány, A. Acetylene hydrogenation on SiO₂ supported gold nanoparticles. *React. Kinet. Catal. Lett.* **2009**, *96*, 43–54. [CrossRef]
38. Masoud, N.; Delannoy, L.; Schaink, H.; van der Eerden, A.; de Rijk, J.W.; Silva, T.A.G.; Banerjee, D.; Meeldijk, J.D.; de Jong, K.P.; Louis, C.; et al. Superior stability of Au/SiO₂ compared to Au/TiO₂ catalysts for the selective hydrogenation of butadiene. *ACS Catal.* **2017**, *7*, 5594–5603. [CrossRef] [PubMed]
39. Drug Topics, Overview of pharmaceutical excipients used in tablets and capsules. Available online: <http://www.drugtopics.com/hospitalhealth-system-pharmacy/overview-pharmaceutical-excipients-used-tablets-and-capsules> (accessed on 26 January 2019).
40. Electronic Code of Federal Regulations, Sec. 172.480, Silicon dioxide. Available online: https://www.ecfr.gov/cgi-bin/text-idx?SID=3d16e9d0330caded75fa66babfa8e949&mc=true&node=se21.3.172_1480&rgn=div8 (accessed on 26 January 2019).
41. Shakeel, M.; Jabeen, F.; Shabbir, S.; Asghar, M.S.; Khan, M.S.; Chaudhry, A.S. Toxicity of nano-titanium dioxide (TiO₂-NP) through various routes of exposure: A review. *Biol. Trace Elem. Res.* **2016**, *172*, 1–36. [CrossRef] [PubMed]

